Chemical Science

ROYAL SOCIETY OF CHEMISTRY

EDGE ARTICLE

View Article Online
View Journal | View Issue

Cite this: *Chem. Sci.*, 2022, **13**, 573

All publication charges for this article have been paid for by the Royal Society of Chemistry

Multivalent supramolecular assembly with ultralong organic room temperature phosphorescence, high transfer efficiency and ultrahigh antenna effect in water†

Wei-Lei Zhou,[ab] Wenjing Lin,[a] Yong Chen,[a] Xian-Yin Dai,[a] Zhixue Liu[a] and Yu Liu *[a]

Received 25th October 2021
Accepted 24th November 2021

DOI: 10.1039/d1sc05861d

rsc.li/chemical-science

Multivalent supramolecular assemblies have recently attracted extensive attention in the applications of soft materials and cell imaging. Here, we report a novel multivalent supramolecular assembly constructed from 4-(4-bromophenyl)pyridine-1-ium bromide modified hyaluronic acid (HABr), cucurbit[8]uril (CB[8]) and laponite® clay (LP), which could emit purely organic room-temperature phosphorescence (RTP) with a phosphorescence lifetime of up to 4.79 ms in aqueous solution *via* multivalent supramolecular interactions. By doping the organic dyes rhodamine B (RhB) or sulfonated rhodamine 101 (SR101) into the HABr/CB[8]/LP assembly, phosphorescence energy transfer was realized with high transfer efficiency (energy transfer efficiency = 73–80%) and ultrahigh antenna effect (antenna effect value = 308–362) within the phosphorescent light harvesting system. Moreover, owing to the dynamic nature of the noncovalent interactions, a wide-range spectrum of phosphorescence energy transfer outputs could be obtained not only in water but also on filter paper and a glass plate by adjusting the donor–acceptor ratio and, importantly, white-light emission was obtained, which could be used in the application of information encryption.

Introduction

Purely organic room-temperature phosphorescence (RTP) with a long lifetime, large Stokes shift, and the involvement of triplet states has attracted increasing attention in bioimaging,[1] anti-counterfeiting materials,[2] organic light-emitting diodes,[3] and so on. However, most purely organic RTP emissions have been shown in the solid-state but are fairly rare in water, owing to the quenching of the collision by the high concentration of dissolved oxygen in water, as well as the free molecular motions for the non-radiative decay process,[4] which inevitably limit their practical biological applications. Thus, it is urgently essential for purely organic RTP in aqueous solution to be developed. In order to improve the yield and lifetime of phosphorescence in aqueous solution, many efforts have been made to study purely organic RTP. The introduction of heavy atoms and rigid environments can avoid the influence of quenchers, suppress the non-radiative decay and increase the intersystem crossing (ISC) for a high phosphorescence quantum yield and long lifetime in water. Among them, the supramolecular strategy through non-covalent interactions (*i.e.* host–guest interaction, hydrogen bonding, π–π stacking) has attracted ever-growing attention in photochemistry because it can affect the electron distribution to alter the optical properties of luminophores.[5] In particular, macrocyclic supramolecular systems are more attractive because purely organic RTP can be realized in water through the host–guest interactions between macrocyclic compounds and luminophores.[4,6]

As a water-soluble biocompatible macrocyclic host compound, cucurbituril (CB) has a stronger binding ability towards positively charged guest molecules than other macrocyclic host compounds, owing to the strong charge dipole, hydrogen bonding and the hydrophobic/hydrophilic interactions that can protect and immobilize the phosphor guests to improve their luminescent efficiency and lifetime in water.[1d,6,7] For example, Tian and Ma *et al.* reported a visible-light excited aqueous purely organic RTP system *via* a supramolecular assembly between CB[8] and a 4-(4-bromophenyl)-pyridine derivative modified triazine to achieve a multicolor transition through changing the host–guest ratios in aqueous solution and hydrogels.[1d] Ma *et al.* constructed a circularly polarized RTP two-arm supramolecular polymer[8] and a three-arm supramolecular RTP organic framework[9] in water by the host–guest interaction of CB[8] with 4-(4-bromophenyl)-pyridin-1-ium modified chiral cyclohexane and benzoate derivatives. We

[a]College of Chemistry, State Key Laboratory of Elemento–Organic Chemistry, Nankai University, People's Republic of China. E-mail: yuliu@nankai.edu.cn

[b]College of Chemistry and Materials Science, Inner Mongolia Key Laboratory of Chemistry for Nature Products and Synthesis for Functional Molecules, Inner Mongolia Minzu University, Tongliao, 028000, People's Republic of China

† Electronic supplementary information (ESI) available. See DOI: 10.1039/d1sc05861d

used bromopyridine salt derivatives as guests and macrocycles CB[6–8] as hosts to construct a series of supramolecular assemblies with ultralong phosphorescence lifetimes and ultrahigh quantum yields in either the solid-state[10–13] or aqueous solution, exhibiting application potential in up-conversion targeted tumor cell imaging,[14] phosphorescent light harvesting energy transfer cell imaging,[15] photo-oxidation driven dual organelle imaging,[16] and antibiotic sensing.[17]

On the other hand, multivalent assembly can effectively improve the yield and lifetime of RTP in aqueous solution. George *et al.* realized red purely organic RTP emission in aqueous solution through laponite® clay (LP) and brominated naphthalene diimide (NDI) phosphor derivatives.[18] In addition, they also achieved aqueous phosphorescence RTP with an ultrahigh quantum yield through LP and a bromo-substituted phthalimide derivative, presenting the effective light harvesting energy transfer from triplet to singlet with the dyes sulforhodamine G (SRG) and sulforhodamine 101 (SR101).[19] However, there have been few reports on the construction of phosphorescent supramolecular systems with high efficiency energy transfer through the multivalent assembly of macrocyclic compounds. Herein, considering the efficient utilization of light energy in light harvesting systems for excellent optical properties,[20] we combined 4-(4-bromophenyl)pyridine-1-ium bromide (BrBP) modified hyaluronic acid (HA), CB[8] and LP to construct a multivalent supramolecular assembly (Fig. 1). This kind of multivalent supramolecular assembly not only showed good phosphorescence properties in water, owing to the electrostatic interactions between the positively charged edges of LP and the negatively charged HABr/CB[8] supramolecular polymer by restricting the non-radiative transition, but also achieved significant phosphorescence light harvesting properties with a high energy transfer efficiency (>73%), ultrahigh antenna effect (>308), and ultralong lifetime (millisecond second level) after associating with the dyes rhodamine B (RhB) or SR101. It is meaningful that adjusting the donor/acceptor ratios can give broad-spectrum multicolor outputs, including white-light emission, in solution as well as on filter paper and a glass plate, which provides a new approach for the development of water-phase RTP.

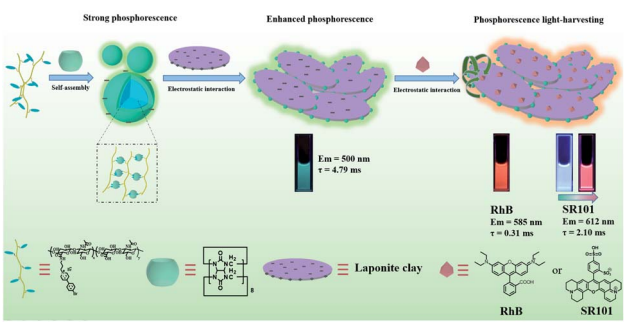

Fig. 1 Schematic illustration of the construction of RTP light harvesting by the multivalent supramolecular assembly HABr/CB[8]/LP with RhB or SR101 in aqueous solution.

Experimental

Materials and methods

All chemicals were obtained from commercial suppliers unless noted otherwise. 4-(4-Bromophenyl)pyridine was purchased from Bide Pharmatech, and 3-bromopropan-1-amine was purchased from Struchem Co. LP was purchased from BYK Additives Inc. NMR spectra were recorded on a Bruker AV400 spectrometer. Fluorescence spectra were recorded in a conventional quartz cell (light path: 10 mm) on a Varian Cary Eclipse spectrophotometer equipped with a Varian Cary single-cell Peltier accessory to control the temperature. UV–vis spectra and optical transmittance were recorded in a quartz cell (light path: 10 mm) on a Shimadzu UV-3600 spectrophotometer equipped with a PTC-348WI temperature controller. Steady-state fluorescence emission spectra were recorded in a conventional quartz cell (10 × 10 × 45 mm) at 298 K on a Varian Cary Eclipse spectrophotometer equipped with a Varin Cary single-cell Peltier accessory to control the temperature. Fluorescence and phosphorescence lifetimes were measured by means of time-correlated single-photon counting on a FLS980 instrument (Edinburgh Instruments, Livingston, UK). High-resolution transmission electron microscopy images were acquired using a Tecnai 20 high-resolution transmission electron microscope operating at an accelerating voltage of 200 keV. The sample was prepared by dropping the solution onto a copper grid, which was then air-dried. Scanning electron microscopy images were obtained with a Hitachi S-3500N scanning electron microscope. The zeta potentials were determined on a NanoBrook 173Plus at 298 K.

Calculation of the energy transfer efficiency (Φ_{ET}) and antenna effect

The energy transfer efficiency (Φ_{ET}) is the ratio of the absorbed energy transferred to the acceptor given by the spectrometric titration experiments, that is, the ratio of the luminescence intensity of the donor when the acceptor is absent and is present (I_D and I_{DA}) (according to the donor: 500 nm and RhB acceptor: 585 nm, SR101 acceptor: 612 nm).

$$\Phi_{ET} = 1 - I_{DA}/I_D$$

At a certain concentration of donor and acceptor, the antenna effect is equal to the ratio of the emission intensity of the acceptor at the corresponding maximum emission upon excitation of the donor. $I_{D+A(\lambda Dex)}$ represents the luminescence intensity of the system under the excitation of the donor in the presence of an acceptor, I_D represents the luminescence intensity of donor under the excitation of the donor and $I_{D+A(\lambda Aex)}$ represents the luminescence intensity of system under the excitation of the acceptor in the presence of the acceptor.

$$\text{Antenna effect} = (I_{D+A(\lambda Dex)} - I_{D(\lambda Dex)})/I_{D+A(\lambda Aex)}$$

Preparation of the HABr/CB[8]/LP assembly

A certain amount of HABr was dissolved in deionized water, then an equivalent amount of CB[8] was added into the above aqueous solution according to the calculation of the concentration using 4-(4-bromophenyl) pyridine-1-ium salt as a standard. Then, a certain amount of LP was added into the prepared assembly to construct the ternary assembly.

Results and discussion

4-(4-Bromophenyl)pyridine-1-ium bromide modified hyaluronic acid (250 kDa) polymer (HABr) was synthesized according to our previous report[14] (Scheme 1), in which the substitution degree of the 4-(4-bromophenyl) pyridine-1-ium bromide phosphors was measured as 3.5% by means of ^{1}H NMR. The binding ratio between CB[8] and the HABr precursor, 1-(3-aminopropyl)-4-(4-bromophenyl)pyridine-1-ium bromide hydrobromide (BrBP-NH_2), was measured as 1 : 2, and the binding constant was up to $(1.09 \pm 0.01) \times 10^{12}$ M^{-2} *via* isothermal titration calorimetry (ITC) experiments. This strong 1 : 2 binding of CB[8] with BrBP-NH_2 demonstrated that CB[8] could strongly associate with the BrBP units in HABr, leading to the formation of a stable supramolecular cross-linked polymer HABr/CB[8]. Like our previous reports, the HABr/CB[8] supramolecular cross-linked polymer emitted strong phosphorescence at 500 nm with a long lifetime of 4.42 ms and a phosphorescence quantum yield of 1.95%, attributed to the cooperative contribution of the charge dipole, π–π stacking, hydrogen bonding interactions and hydrophobic/hydrophilic effect between CB[8] and BrBP, as well as the multiple hydrogen bonds from HA, which avoided the attack of oxygen and other molecules in aqueous solution, suppressed molecular rotation and enhanced the ISC efficiently.[14] The zeta potentials of HABr, LP, HABr/CB[8] and HABr/CB[8]/LP were measured as −74 mV, −32 mV, −39 mV and −51.4 mV, respectively (Fig. S1†), indicating that the surface of HABr/CB[8] was negatively charged and had the potential to interact with the positively charged substrate. In addition, the zeta potential of HABr/CB[8]/LP is higher than the sum of those of HABr/CB[8] and LP under the same conditions, indicating that HABr/CB[8] may interact with the positively charged edges of LP. In addition, after adding LP that had been neutralized by adding the ionic polymer chains sodium polyacrylate or sodium alginate (Fig. S2†) to the supramolecular cross-linked polymer HABr/CB[8], the phosphorescence intensity did not increase but decreased to a certain extent, further demonstrating that the interaction between the ionic HABr/CB[8] and the cationic edge of LP is beneficial to the enhancement of the phosphorescence.

UV–vis and phosphorescence spectra were used to investigate the changes in the optical properties after adding LP into the supramolecular cross-linked polymer HABr/CB[8]. The UV–vis spectrum of free HABr showed an absorption maximum at 300 nm. After the addition of CB[8], this absorption maximum red-shifted 5 nm, accompanied by a decrease of the absorption intensity and the appearance of two isosbestic points at 250 nm and 325 nm, indicating the formation of the supramolecular cross-linked polymer HABr/CB[8] (Fig. 2a). After further adding the LP clay (0.02 wt%) to HABr/CB[8], the absorption intensity was enhanced to a certain extent, and no shift of the absorption maximum was observed. Interestingly, the addition of LP clay increased the original phosphorescence intensity, phosphorescence lifetime and phosphorescence quantum yield of HABr/CB[8] by 1.6 times, 1.1 times and 1.9 times, respectively (Fig. 2b–d, S3 and S4†), giving a ultralong phosphorescence lifetime of up to 4.79 ms and a phosphorescence quantum yield of up to 3.79%. A possible reason for the improved RTP may be as follows: LP has a unique double-charged structure with a negatively charged surface and positively charged edges.[18,19] Therefore, the negatively charged supramolecular cross-linked polymer HABr/CB[8] could interact with the positively charge edges of LP, which consequently stabilized HABr/CB[8] *via* electrostatic interactions and, thus, improved the phosphorescence properties. Scanning electron microscopy (SEM) and transmission electron microscopy (TEM) images of HABr/CB[8]/LP showed a number of lamellar aggregates, which was very different from the spherical morphology of HABr/CB[8] (Fig. S5†).

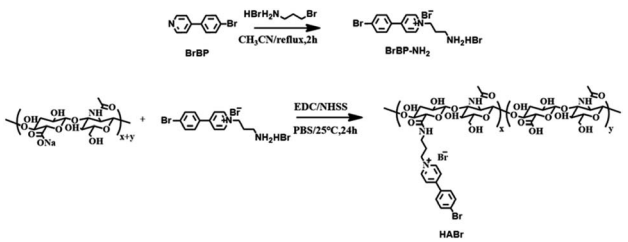

Scheme 1 The synthetic route of HABr.

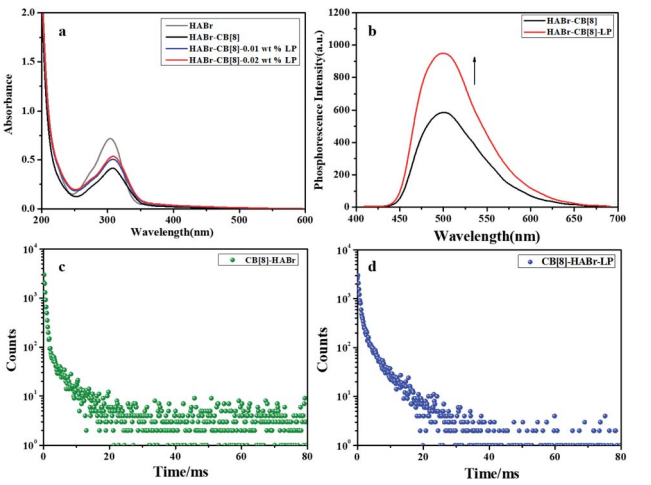

Fig. 2 (a) Absorption spectra of free HABr (0.05 mM, grey), HABr/CB[8] ([CB[8]] = 0.025 mM, black), HABr/CB[8]/LP ([LP] = 0.01 wt%, blue) and HABr/CB[8]/LP ([LP] = 0.02 wt%, red) in water at 298 K; (b) phosphorescence spectra (delayed by 0.2 ms, E_x, slit = 5 nm; E_m, slit = 10 nm) of HABr/CB[8] (black) and HABr/CB[8]/LP (red) ([HABr] = 0.1 mM, [CB[8]] = 0.05 mM, [LP] = 0.02 wt%) in water at 298 K (λ_{ex} = 300 nm); the phosphorescence decay curves of (c) HABr/CB[8] and (d) HABr/CB[8]/LP at 500 nm at 298 K.

Energy transfer from a long-lived phosphor to a short-lived fluorophore is an effective way to achieve long-lived fluorescence,[19,21] but efficient phosphorescence light harvesting systems in aqueous solution are still rare. In the present research, we constructed a multivalent supramolecular assembly to provide a suitable platform for efficient phosphorescent light harvesting energy transfer. Based on the good overlap between the UV–vis absorption of RhB and the phosphorescence emission of HABr/CB[8]/LP (Fig. 3a), we selected HABr/CB[8]/LP as the donor and RhB or SR101 as the acceptors for energy transfer. As shown in Fig. 3b, with the addition of RhB, the phosphorescence peak of HABr/CB[8]/LP at 500 nm gradually decreased, and the fluorescence peak of RhB gradually increased at 585 nm in water when excited at 300 nm. In time-resolved decay experiments, the lifetime of the phosphorescence emission of HABr/CB[8]/LP/RhB at 500 nm in aqueous solution decreased from 4.42 ms to 1.00 ms at a D/A ratio of 25 : 1 (Fig. 4a and S6a†), but the lifetime of the fluorescence emission at 585 nm was measured as 0.31 ms, which was much longer than that of free RhB (1.58 ns, Fig. 4b, S7 and c†). These results indicated the phosphorescence energy resonance transfer from the triplet state of HABr/CB[8]/LP (donor) to the singlet state of RhB (acceptor), leading to the delayed fluorescence of RhB. The energy transfer efficiency (Φ_{ET}) and antenna effect are the two main parameters to evaluate the effectiveness

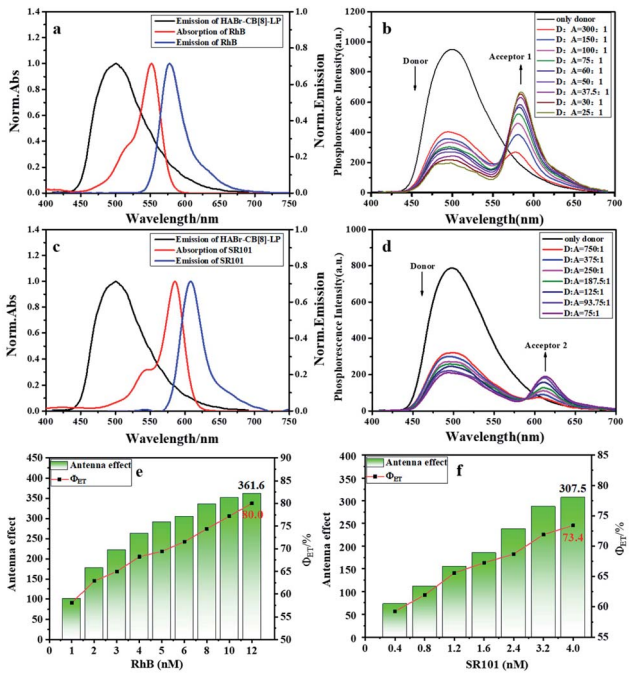

Fig. 3 Normalized emission spectrum of HABr/CB[8]/LP and the absorption and emission spectra of (a) RhB and (c) SR101. Phosphorescence spectrum (delayed by 0.2 ms) of HABr/CB[8]/LP in aqueous solution with different concentrations of (b) RhB and (d) SR101. The antenna effect/Φ_{ET} of HABr/CB[8]/LP in aqueous solution with different concentrations of (e) RhB (according to emission of the donor: 500 nm, acceptor 1 : 585 nm); (f) SR101 (according to emission of the donor: 500 nm, acceptor 2 : 612 nm). ([HABr] = 0.1 mM, [CB[8]] = 0.05 mM, LP = 0.02 wt%, λ_{ex} = 300 nm, 298 K).

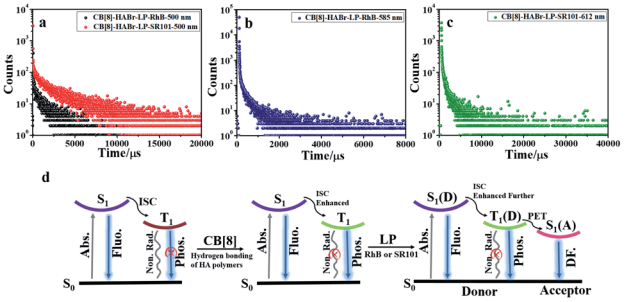

Fig. 4 Time-resolved PL decay curves of (a) HABr/CB[8]/LP/RhB and HABr/CB[8]/LP/SR101 at 500 nm, (b) HABr/CB[8]/LP/RhB at 585 nm and (c) HABr/CB[8]/LP/SR101 at 612 nm in aqueous solution at 298 K. ([HABr] = 0.1 mM, [CB[8]] = 0.05 mM, LP = 0.02 wt%, [RhB] = 4.0 × 10^{-6} M, [SR101] = 1.3 × 10^{-6} M, λ_{ex} = 300 nm, 298 K). (d) A possible diagram of the mechanism of the RTP energy transfer process for the HABr/CB[8]/LP/RhB and HABr/CB[8]/LP/SR101 systems (abs. = absorption, fluo. = fluorescence, non. rad. = non-radiation, ISC = intersystem crossing, phos. = phosphorescence, PET = phosphorescence energy transfer, DF. = delayed fluorescence).

of light harvesting.[20,22] The energy transfer efficiency quantifies the changes of the donor emission intensity in the presence of different concentrations of the acceptor. The antenna effect is a parameter of the acceptor emission changes under different donor concentrations, and is an empirical measurement of the light harvesting efficiency in the system. A high antenna effect represents significantly enhanced emission after absorbing more incident light. Furthermore, the energy transfer efficiency (Φ_{ET}) and antenna effect value of the HABr/CB[8]/LP/RhB system were calculated using a previously reported method.[20,22] From the spectral titration experiments, when the donor–acceptor ratio was 25 : 1, the energy transfer efficiency of the system reached 80%, and the antenna effect value was 361.6 (Fig. 3e, S8a and b†). To the best of our knowledge, these values are the highest organic phosphorescent transfer efficiency and antenna effect values compared to other work (Table S1†),[23,24] especially in aqueous systems. In addition, in order to investigate the universality of the multivalent supramolecular cross-linked polymer platform for phosphorescence energy transfer, we also selected SR101 as another acceptor, whose absorption coincided with the phosphorescence emission of HABr/CB[8]/LP (Fig. 3c). When SR101 was gradually added into HABr/CB[8]/LP, the phosphorescence of HABr/CB[8]/LP at 500 nm gradually decreased, and the emission peak at 612 nm gradually increased (Fig. 3d). At a D/A ratio of 75 : 1, the transfer efficiency reached 73.4% and the antenna effect value reached 307.5 (Fig. 3f, S8c and d†). The phosphorescence lifetime (at 500 nm) of HABr/CB[8]/LP decreased from 4.42 ms to 3.01 ms, and the fluorescence lifetime of SR101 at 612 nm increased from 4.91 ns to 2.10 ms (Fig. 4a, c, S6b, S7b and d†). In the control experiments (Fig. S9d†), no phosphorescent emission could be observed in the case of free RhB or SR101 when excited at 300 nm under the same conditions, and HABr/CB[8]/LP showed no phosphorescence emission when excited at the absorption maximum of RhB (550 nm) or SR101(580 nm), as shown in Fig. S8b and d.† Without LP, the antenna effect values of HABr/

CB[8]/RhB or HABr/CB[8]/SR101 were only 11.7 and 4.6 respectively, which were 31 times and 67 times lower, respectively, than that of the assembly with LP, accompanied by a decrease in the transfer efficiency by 61.0% for HABr/CB[8]/RhB and 40.3% for HABr/CB[8]/SR101 (Fig. S9 and S10†). These lower energy transfer efficiencies also verified the critical role of LP in interacting with both the donor and the acceptor. These results demonstrated that the multivalent assembly played an important role in the phosphorescence energy transfer and light harvesting. A possible mechanism is illustrated in Fig. 4d, where the electrostatic interaction between the positively charged edges of LP and the negatively charged phosphorescent supramolecular polymer restricted the non-radiative transition of the phosphorescent group and reduced the collision with oxygen in water to a certain extent. On the other hand, the remaining negatively charged surface of LP generated electrostatic interactions with the cationic dyes, thus shortening the distance between the donor and acceptor and leading to the efficient and long-lived phosphorescent light harvesting energy transfer in water.

Considering the good phosphorescence energy transfer and light harvesting properties of the multivalent supramolecular assembly, we were able to quickly tune the emission color *via* simply adjusting the molar ratio of D/A to achieve wide spectral outputs for multicolor photoluminescence. As shown in Fig. 5, the phosphorescence colors of the hybrid supramolecular assembly aqueous solution changed from green to orange–yellow (for HABr/CB[8]/LP/RhB) or from green to pink (for HABr/CB[8]/LP/SR101) with varying donor/acceptor ratios, and the same trend of color change was also observed on a 2D projection of the CIE (Commission Internationale de l'Eclairage) xy chromaticity diagram. Interestingly, warm white light with color coordinates of 0.33, 0.37 on the CIE diagram was obtained at a D/A molar ratio of 187.5 : 1 in HABr/CB[8]/LP/SR101, which was very close to the exact white point (0.33, 0.33). Significantly, this series of multicolor luminescent aqueous solutions are suitable to be used as luminescent inks. After writing with pre-prepared assembly solutions of HABr/CB[8]/LP, HABr/CB[8]/LP/RhB and HABr/CB[8]/LP/SR101 on ordinary filter paper or a glass plate, multicolor luminescence, including white light emission, could be clearly observed by the naked eye (Fig. 5c and d). In the control experiment, no white light emission could be seen in the case of HABr/CB[8]/SR101 without LP under same conditions (Fig. S11†). The solid-phase luminescence results further verified that the multivalent supramolecular assembly that we constructed could carry out efficient light harvesting energy transfer with dyes to achieve multicolor spectral adjustment. In addition, we investigated the delayed luminescence effect of HABr/CB[8]/LP through the phosphorescence spectra of HABr/CB[8]/LP at different delay times. The phosphorescence emission could still be detected at 4.2 ms after turning off the excitation source, although the afterglow effect could not be captured by the naked eye (Fig. S12†).

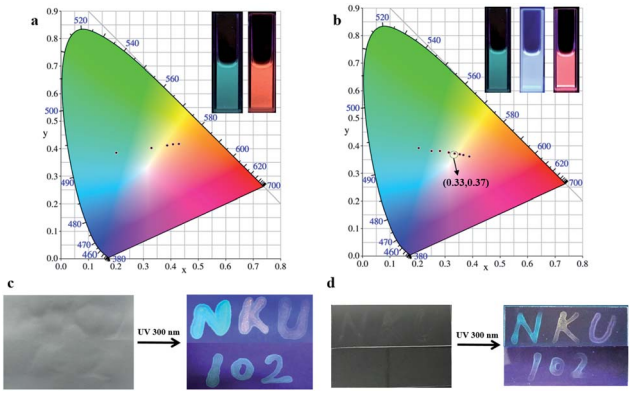

Fig. 5 The CIE chromaticity diagrams of the photoluminescence color changes from varying the ratios of (a) RhB (inset: photographs of HABr/CB[8]/LP and HABr/CB[8]/LP/RhB) and (b) SR101(inset: photographs of HABr/CB[8]/LP, HABr/CB[8]/LP/0.005SR101 and HABr/CB[8]/LP/SR101). The photoluminescence inks based on the light harvesting system: (c) photographs writing "N" with HABr/CB[8]/LP, "K" with HABr/CB[8]/LP/RhB, "U" with HABr/CB[8]/LP/SR101 and "102" with HABr/CB[8]/LP/0.005SR101 (c) on filter paper under natural light and under UV light; (d) doped PVA on glass under natural light and under UV light.

Conclusions

In conclusion, we constructed a new multivalent phosphorescent light harvesting supramolecular assembly through host–guest and electrostatic interactions based on HABr, CB[8] and LP, which showed a long phosphorescence lifetime (4.79 ms) and satisfactory quantum yield (3.79%) in water. Furthermore, by virtue of the multivalent supramolecular cross-linked polymer acting as the phosphorescence donor and the dyes RhB or SR101 as the acceptors, the resultant system could realize a high phosphorescence energy efficiency (73–80%) and ultrahigh antenna effect value (308–362) in water. By adjusting the D/A ratio, a wide range of multicolor emissions could be achieved in aqueous solution, as well as on filter paper and a glass plate. This strategy of combining purely RTP and a multivalent assembly may provide an effective way to develop water-phase phosphorescence and further their applications in biology and displays.

Data availability

The data that support the findings of this study are available from the corresponding author upon reasonable request.

Author contributions

Y. L., Y. C., and W.-L. Z. conceived and designed the experiments. W.-L. Z. and W. L. synthesized and performed the chemical characterization. W.-L. Z. wrote the main manuscript. Y. L. supervised the work and edited the manuscript. All authors analyzed and discussed the results and reviewed the manuscript.

Conflicts of interest

There are no conflicts to declare.

Acknowledgements

This work was supported by the National Natural Science Foundation of China (22101143, 22131008 and 21971127), the China Postdoctoral Science Foundation (2021M691661) and the National Natural Science Foundation of Inner Mongolia (2021BS02014).

Notes and references

1 (*a*) S. M. A. Fateminia, Z. Mao, S. Xu, Z. Yang, Z. Chi and B. Liu, *Angew. Chem., Int. Ed.*, 2017, **56**, 12160–12164; (*b*) J. Yang, Z. Xu, B. Wang, X. Gao, Z. Ren, J. Wang, Y. Xie, J. Li, Q. Peng, K. Pu and Z. Li, *Nat. Commun.*, 2018, **9**, 840; (*c*) X. Jia, C. Shao, X. Bai, Q. Zhou, B. Wu, L. Wang, B. Yue, H. Zhu and L. Zhu, *Proc. Natl. Acad. Sci. U. S. A.*, 2019, **116**, 4816–4821; (*d*) J. Wang, Z. Huang, X. Ma and H. Tian, *Angew. Chem., Int. Ed.*, 2020, **59**, 9928–9933; (*e*) X.-Q. Liu, K. Zhang, J.-F. Gao, Y.-Z. Chen, C.-H. Tung and L.-Z. Wu, *Angew. Chem., Int. Ed.*, 2020, **59**, 23456–23460; (*f*) Q. Dang, Y. Jiang, J. Wang, J. Wang, Q. Zhang, M. Zhang, S. Luo, Y. Xie, K. Pu, Q. Li and Z. Li, *Adv. Mater.*, 2020, **32**, 2006752.

2 (*a*) S. Cai, H. Shi, D. Tian, H. Ma, Z. Cheng, Q. Wu, M. Gu, L. Huang, Z. An, Q. Peng and W. Huang, *Adv. Funct. Mater.*, 2018, **28**, 1705045; (*b*) Y. Su, S. Z. F. Phua, Y. Li, X. Zhou, D. Jana, G. Liu, W. Q. Lim, W. K. Ong, C. Yang and Y. Zhao, *Sci. Adv.*, 2018, **4**, eaas9732; (*c*) X. Zhang, L. Du, W. Zhao, Z. Zhao, Y. Xiong, X. He, P. F. Gao, P. Alam, C. Wang, Z. Li, J. Leng, J. Liu, C. Zhou, J. W. Y. Lam, D. L. Phillips, G. Zhang and B. Z. Tang, *Nat. Commun.*, 2019, **10**, 5161; (*d*) X. Yao, J. Wang, D. Jiao, Z. Huang, O. Mhirsi, F. Lossada, L. Chen, B. Haehnle, A. J. C. Kuehne, X. Ma, H. Tian and A. Walther, *Adv. Mater.*, 2021, **33**, 2005973; (*e*) H. Wu, W. Chi, Z. Chen, G. Liu, L. Gu, A. K. Bindra, G. Yang, X. Liu and Y. Zhao, *Adv. Funct. Mater.*, 2019, **29**, 1807243; (*f*) L. Gu, H. Wu, H. Ma, W. Ye, W. Jia, H. Wang, H. Chen, N. Zhang, D. Wang, C. Qian, Z. An, W. Huang and Y. Zhao, *Nat. Commun.*, 2020, **11**, 944; (*g*) L. Gu, W. Ye, X. Liang, A. Lv, H. Ma, M. Singh, W. Jia, Z. Shen, Y. Guo, Y. Gao, H. Chen, D. Wang, Y. Wu, J. Liu, H. Wang, Y.-X. Zheng, Z. An, W. Huang and Y. Zhao, *J. Am. Chem. Soc.*, 2021, **143**, 18527–18535; (*h*) J. Yang, M. Fang and Z. Li, *Acc. Mater. Res.*, 2021, **2**, 644–654.

3 (*a*) Q. Zhang, B. Li, S. Huang, H. Nomura, H. Tanaka and C. Adachi, *Nat. Photonics*, 2014, **8**, 326–332; (*b*) R. Kabe, N. Notsuka, K. Yoshida and C. Adachi, *Adv. Mater.*, 2016, **28**, 655–660; (*c*) Q. Li and Z. Li, *Acc. Chem. Res.*, 2020, **53**, 962–973.

4 (*a*) X. Ma, J. Wang and H. Tian, *Acc. Chem. Res.*, 2019, **52**, 738–748; (*b*) W. Zhao, Z. He and B. Z. Tang, *Nat. Rev. Mater.*, 2020, **5**, 869–885; (*c*) T. Zhang, X. Ma, H. Wu, L. Zhu, Y. Zhao and H. Tian, *Angew. Chem., Int. Ed.*, 2020, **59**, 11206–11216; (*d*) Z. Huang and X. Ma, *Cell Rep. Phys. Sci.*, 2020, **1**, 100167.

5 (*a*) S. Datta, M. L. Saha and P. J. Stang, *Acc. Chem. Res.*, 2018, **51**, 2047–2063; (*b*) Y. Ai, M. H. Chan, A. K. Chan, M. Ng, Y. Li and V. W. Yam, *Proc. Natl. Acad. Sci. U. S. A.*, 2019, **116**, 13856–13861; (*c*) Y. Zhang, Y. Su, H. Wu, Z. Wang, C. Wang, Y. Zheng, X. Zheng, L. Gao, Q. Zhou, Y. Yang, X. Chen, C. Yang and Y. Zhao, *J. Am. Chem. Soc.*, 2021, **143**, 13675–13685; (*d*) W.-L. Zhou, Y. Chen and Y. Liu, *Acta Chim. Sin.*, 2020, **78**, 1164–1176; (*e*) W.-L. Zhou, Y. Chen, W. Lin and Y. Liu, *Chem. Commun.*, 2021, **57**, 11443–11456; (*f*) W. Zhou, Y. Chen, Q. Yu, P. Li, X. Chen and Y. Liu, *Chem. Sci.*, 2019, **10**, 3346–3352.

6 (*a*) Y. Chen, F. Huang, Z.-T. Li and Y. Liu, *Sci. China: Chem.*, 2018, **61**, 979–992; (*b*) P.-Y. Li, Y. Chen and Y. Liu, *Chin. Chem. Lett.*, 2019, **30**, 1190–1197; (*c*) W.-L. Zhou, X. Zhao, Y. Chen and Y. Liu, *Org. Chem. Front.*, 2019, **6**, 10–14; (*d*) D. Dai, Z. Li, J. Yang, C. Wang, J. Wu, Y. Wang, D. Zhang and Y.-W. Yang, *J. Am. Chem. Soc.*, 2019, **141**, 4756–4763; (*e*) X. Yu, W. Liang, Q. Huang, W. Wu, J.-J. Chruma and C. Yang, *Chem. Commun.*, 2019, **55**, 3156–3159.

7 (*a*) G. Yu, K. Jie and F. Huang, *Chem. Rev.*, 2015, **115**, 7240–7303; (*b*) S. J. Barrow, S. Kasera, M. J. Rowland, J. d. Barrio and O. A. Scherman, *Chem. Rev.*, 2015, **115**, 12320–12406; (*c*) L. Xu, L. Zou, H. Chen and X. Ma, *Dyes Pigm.*, 2017, **142**, 300–305; (*d*) Y. Gong, H. Chen, X. Ma and H. Tian, *ChemPhysChem*, 2016, **17**, 1934–1938.

8 C. Xu, C. Yin, W. Wu and X. Ma, *Sci. China: Chem.*, 2021, DOI: 10.1007/s11426-021-1104-9.

9 C. Xu, X. Lin, W. Wu and X. Ma, *Chem. Commun.*, 2021, **57**, 10178–10181.

10 Z.-Y. Zhang, Y. Chen and Y. Liu, *Angew. Chem., Int. Ed.*, 2019, **58**, 6028–6032.

11 Z.-Y. Zhang and Y. Liu, *Chem. Sci.*, 2019, **10**, 7773–7778.

12 Z.-Y. Zhang, W.-W. Xu, W.-S. Xu, J. Niu, X.-H. Sun and Y. Liu, *Angew. Chem., Int. Ed.*, 2020, **59**, 18748–18754.

13 X.-K. Ma, W. Zhang, Z. Liu, H. Zhang, B. Zhang and Y. Liu, *Adv. Mater.*, 2021, **33**, 2007476.

14 W.-L. Zhou, Y. Chen, Q. Yu, H. Zhang, Z. Liu, X. Dai, J. Li and Y. Liu, *Nat. Commun.*, 2020, **11**, 4655.

15 F.-F. Shen, Y. Chen, X. Dai, H.-Y. Zhang, B. Zhang, Y.-H. Liu and Y. Liu, *Chem. Sci.*, 2021, **12**, 1851–1857.

16 H.-J. Yu, Q. Zhou, X. Dai, F.-F. Shen, Y.-M. Zhang, X. Xu and Y. Liu, *J. Am. Chem. Soc.*, 2021, **143**, 13887–13894.

17 D.-A. Xu, Q.-Y. Zhou, X. Dai, X.-K. Ma, Y.-M. Zhang, X. Xu and Y. Liu, *Chin. Chem. Lett.*, 2021, DOI: 10.1016/j.cclet.2021.08.001.

18 S. Kuila, K. V. Rao, S. Garain, P. K. Samanta, S. Das, S. K. Pati, M. Eswaramoorthy and S. J. George, *Angew. Chem., Int. Ed.*, 2018, **57**, 17115–17119.

19 S. Garain, B. C. Garain, M. Eswaramoorthy, S. K. Pati and S. J. George, *Angew. Chem., Int. Ed.*, 2021, **60**, 19720–19724.

20 (*a*) G. D. Scholes, G. R. Fleming, A. Olaya-Castro and R. van Grondelle, *Nat. Chem.*, 2011, **3**, 763–774; (*b*) X. Zhu, J. X. Wang, L. Y. Niu and Q. Z. Yang, *Chem. Mater.*, 2019, **31**, 3573–3581; (*c*) P. Wang, X. Miao, Y. Meng, Q. Wang, J. Wang, H. Duan, Y. Li, C. Li, J. Liu and L. Cao, *ACS Appl. Mater. Interfaces*, 2020, **12**, 22630–22639; (*d*) J.-J. Li, Y. Chen, J. Yu, N. Cheng and Y. Liu, *Adv. Mater.*, 2017, **29**, 1701905; (*e*) M. Hao, G. Sun, M. Zuo, Z. Xu, Y. Chen, X.-Y. Hu and L. Wang, *Angew. Chem., Int. Ed.*, 2020, **59**, 10095–10100; (*f*) H.-Q. Peng, L.-Y. Niu, Y.-Z. Chen,

L.-Z. Wu, C.-H. Tung and Q.-Z. Yang, *Chem. Rev.*, 2015, **115**, 7502–7542.
21 (*a*) S. Kuila and S. J. George, *Angew. Chem., Int. Ed.*, 2020, **59**, 9393–9397; (*b*) Z. Li, Y. Han and F. Wang, *Nat. Commun.*, 2019, **10**, 3735.
22 Z. Xu, S. Peng, Y. Y. Wang, J. K. Zhang, A. I. Lazar and D. S. Guo, *Adv. Mater.*, 2016, **28**, 7666–7671.
23 R. Gao and D. Yan, *Chem. Sci.*, 2017, **8**, 590–599.
24 B. Zhou, Q. Zhao, L. Tang and D. Yan, *Chem. Commun.*, 2020, **56**, 7698–7701.